Resistance welding of carbon fibre reinforced PEKK by means of CNT webs

Journal:	*Journal of Composite Materials*
Manuscript ID	JCM-22-0887.R1
Manuscript Type:	Original Manuscript
Date Submitted by the Author:	n/a
Complete List of Authors:	Russello, Massimiliano; Queen's University Belfast Catalanotti, Giuseppe; Universidade de Évora, School of Science and Technology Hawkins, Stephen; Queen's University Belfast Falzon, Brian; RMIT University
Keywords:	Resistance welding, CNT web, fibre-reinforced thermoplastics, fusion bonding
Abstract:	Single lap shear specimens were manufactured using resistance welding of carbon fibre reinforced substrates by means of CNT web-based heating elements. Heating elements were manufactured by embedding the CNT web layers between layers of PEKK / glass fibre and connecting them to copper electrodes. An experimental campaign explored their electrothermal behaviour influencing the welding process. Single lap shear specimens were then welded at a pressure of 0.05 MPa and different levels of power and duration. An optimum bond was obtained with a specific power of 80-90 kW/m2 and a time of 150 s, achieving a shear strength of 30 MPa. Post-mortem analysis revealed that fracture propagated within the substrates. This work represents a further step in the integration of CNT web-based heating elements in an industrial welding process.

Resistance welding of carbon fibre reinforced PEKK by means of CNT webs

M. Russello[a], G. Catalanotti[a,b,*], S.C. Hawkins[a,c], B.G. Falzon[a,d]

[a] *Advanced Composites Research Group (ACRG), School of Mechanical and Aerospace Engineering, Queen's University Belfast, Belfast BT9 5AH, UK*

[b] *Escola de Ciências e Tecnologia, Universidade de Évora, 7000-671 Évora, Portugal*

[c] *Department of Materials Science and Engineering, Monash University, Clayton 3800, Australia*

[d] *School of Engineering, RMIT University, Melbourne, 3001, Australia*

Abstract

Single lap shear specimens were manufactured using resistance welding of carbon fibre reinforced substrates by means of CNT web-based heating elements. Heating elements were manufactured by embedding the CNT web layers between layers of PEKK / glass fibre and connecting them to copper electrodes. An experimental campaign explored their electrothermal behaviour influencing the welding process. Single lap shear specimens were then welded at a pressure of 0.05 MPa and different levels of power and duration. An optimum bond was obtained with a specific power of 80-90 kW/m^2 and a time of 150 s, achieving a shear strength of 30 MPa. Post-mortem analysis revealed that fracture propagated within the substrates. This work represents a further step in the integration of CNT web-based heating elements in an industrial welding process.

Keywords

Resistance welding; CNT web; fibre-reinforced thermoplastics; fusion bonding.

Introduction

Resistance welding ~~is~~has widely been ~~used~~ studied and developed ~~in the aerospace industry~~ to bond fibre-reinforced thermoplastic polymer (FRTP) components [1,2,11–17,3–10]. The technique entails the use of a conductive ~~susceptor or~~ heating element within or between the closely mating surfaces to be joined. Joule heating ~~of the susceptor~~, together with appropriate consolidation pressure promotes melting and interdiffusion and hence bonding of the surfaces, thereby permanently trapping the ~~susceptor~~heating element.

Several other thermal bonding techniques have been developed for joining thermoplastics with the heat being generated, for example, by ultrasonic, microwave and induction processes [1,4,18]. Each method has both advantages and drawbacks. For example, microwave excitation is a non-contact method but will heat an entire susceptible volume rather than just the mating surface. FRTP composites of conductive fibres such as carbon

*Corresponding author. Tel: +351 266 745 371. Email address: gcatalanotti@uevora.pt (Giuseppe Catalanotti)

(i.e. CFRTP) effectively prevent penetration of this electromagnetic radiation (EMR) and hence this method is not generally suitable for this material [1].

Induction welding entails the use of a coil energised with a high-frequency alternating current to induce eddy currents in a conductive substrate. It is also non-contact and can be used to join large components as the coil can be moved along the bond line [1] without the shielding or guides required by microwaves. However, ~~induction welding is also a bulk or volume heating method and hence can negatively affect the overall material properties. The~~ the technology presents some limitations, for example, to weld smaller features where a uniform temperature is required and it is ~~problematic~~ harder to weld unidirectional CFRTPs because it is difficult to generate eddy currents with this fibre architecture~~. Moreover, the temperature increase is generated within the fibres, and therefore within the bulk of the material. This makes the welding inefficient, especially~~ Also difficulties ~~when~~arise when welding thick parts because the heat is ~~not~~ hard to be generated directly at the bonding interface and could adversely affect the mechanical properties of the laminate (e.g. the crystallinity of the polymer, and therefore the material properties, could change with temperature).

Ultrasonic welding is a contact method, somewhat akin to spot friction welding, and is commonly used in the ~~aerospace~~ plastic industry for repetitive and rapid joining of small thermoplastic parts. It is generally not suitable for large, thick or complex-shaped components [1,4,19] as the sound transmission falls off rapidly with thickness.

Many of the disadvantages of other thermal bonding methods can be avoided with resistance welding which suits a broad variety of thermoplastic materials [3]. As this method heats only the interface to be joined, the energy requirement is minimized; the size, thickness and shape of the parts are of minor effect; and bulk material changes are not a problem. The main challenges are ensuring temperature uniformity within the weld region [20] and preventing current leakage from the element when joining conductive substrates [2,4,20–22]. Consolidation pressure is also a critical parameter to consider, especially when large surfaces need to be welded [23]. Several studies report the use of consolidation pressures in the range 0.15 - 0.20 MPa [4,24,25]. Other works report pressures of 1 MPa [21,26–28]. This means that special care need to be taken when welding larger parts since this would require the use of powerful tools or the adoption of alternative methods such as those involving a moving roller to apply consolidation pressure. ~~This means that when welding large parts powerful tools need to be used.~~

Different types of resistance welding heating elements have been investigated [22,29–33]. These mainly consist of metallic meshes [19,21,22,24,26,28,34] or carbon fibre (CF) material systems (either CF fabrics or CF ‘Organo Sheets’ - CFRTP film preforms) [4,25].

Metallic meshes are relatively heavy, can be affected by or promote corrosion, and can increase the radar cross-section [1]. Moreover, because their surface chemistry and physical properties (e.g. stiffness, thermal conductivity and expansion) are very different to those of carbon fibre, ensuing residual stress can promote cracks at the interface [27,28]. During welding, metallic meshes need to be electrically connected using high-pressure clamps to minimize contact resistance [2,4,19,21]. Pressures between 2 and 16.3 MPa have been reported [4,21,35]. Dubé et al. [28] showed that a smaller wire diameter would reduce its inclusion effect. However, because of the lack of chemical bonding between the metallic mesh and the polymer, physical entanglement is considered as the major, if not only, bonding mechanism at the metal/polymer interface. Efforts to enhance adhesion to the metallic meshes include sandblasting, aryl diazonium grafting, silane grafting [31], organosilane coating [36] and even coating with flame grown carbon nanotubes (CNT) [35].

CFRTP film 'organo' sheets have been studied as heating elements but require thorough removal of the polymer from the electrical connection areas, and high clamping pressure to avoid critical problems such as poor reproducibility [22], and excessive heating at the junctions [25]. Scaling [27], and particularly temperature non-uniformity when using ~~UD~~ unidirectional (UD) organo sheets, are also problematic[22,28].

Carbon nanotubes (CNT) dispersed in the polymer [27] have been proposed as a heating element for thermoplastic joining but encounter the addition of a processing step where the polymer needs to be processed to add the CNTs. We have previously reported studies into the control of electrical conductivity in polymer films and thin layers using both CF grown CNT [37] and, combinations of CF and CNT web [38] with particular emphasis on their use as heating elements [37,38]. We recently reported the use of layers of aligned CNT web alone, each only around 50 nm in thickness, to weld neat thermoplastic objects [39]. CNT web heating elements can be efficiently produced at an industrial scale, are not affected by corrosion, are highly flexible and are of negligible weight. The web, which is comprised of CNT of around 10 nm diameter and 300 µm length, is thin, highly conformable and porous, and, being composed entirely of carbon, highly compatible with thermoplastics, thereby greatly facilitating interpenetration of the interface polymer [35] and thus the inclusion effect of the web within the joint can be mitigated. The flexibility of the CNT web allows the welding of complex mating surfaces. The electrical connections between the electrodes and the CNT web do not require clamping or high-pressure tools [39]. We now report the use of CNT web heating elements for joining thermoplastic parts with carbon fibre reinforcement (CFRTP) The welding of aerospace-grade carbon fibre (CF) reinforced polyether ketone ketone (PEKK) polymer matrix is demonstrated and aspects of the proposed technology are investigated to facilitate application in an industrial environment.

1 Materials and methods

1.1 Specimen manufacturing

Standard single-lap shear test samples were produced by welding two CFRTP specimens using the CNT heating elements, and studying both the welding process and the mechanical performance of the welded joints.

Heating elements were produced by sandwiching 10 layers of carbon nanotube web (hereinafter indicated with CNTW10) between PEKK films (nominal thickness of 50 μm). Two types of heating elements were prepared comprising either: i) PEKK/CNTW10/PEKK (denoted HEP); or ii) G/PEKK/PEKK/CNTW10/PEKK/PEKK/G (denoted HEG), where G indicates plain weave of glass fibre fabric having an areal weight of 25 or 50 g/m^2 ~~gsm~~ as indicated in the text. Glass fabric was studied as a means to prevent current leakage from the CNT web in the latter stages of the welding process.

The highly aligned 100 mm wide CNT web was drawn from a forest grown on a silicon wafer, laid on a PEKK film 300 mm long (Fig. 1a) and densified using acetone (Fig. 1b). The acetone densification improves the compactness of the web, reducing the thickness of the single CNT web layer from 20 μm to 50 nm, making the web cling to the PEKK and hence easier to handle.

The film bearing the CNT web layers was then cut into 30 mm × 100 mm strips across the longitudinal direction of the web. Copper electrodes (10 mm x 100 mm) were attached along the long edges of each strip by means of silver paint to leave around a 20 mm wide clear CNT zone.
A second film of PEKK placed on top of the CNT web layers yielded the HEP assembly shown in Fig. 2a. Sandwiching the CNT web and PEKK carrier between PEKK films and glass fabric yielded the HEG assembly in Fig. 2b. These assemblies were consolidated in a vacuum bag at -95 kPa while the temperature was increased to 370°C over 280s; held above the PEKK melting temperature (343°C) for 1 or 4 minutes (for HEP or HEG, respectively); and allowed to cool naturally to <100 °C (approximately 20 min). Finally, the consolidated element was cut into smaller pieces of 25 mm (Fig. 3).

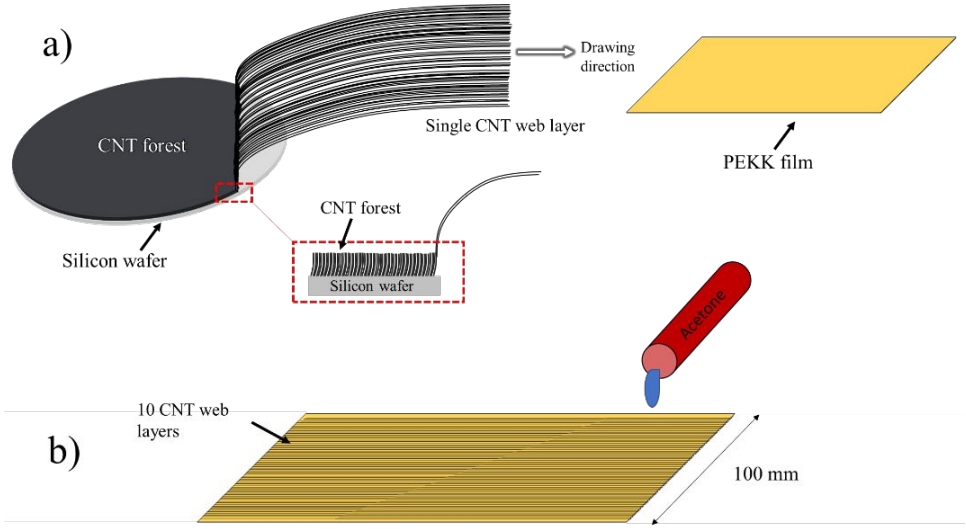

Figure 1 – a) Drawing process of CNT web layers from the CNT forest to the PEKK film and b) densification process using acetone.

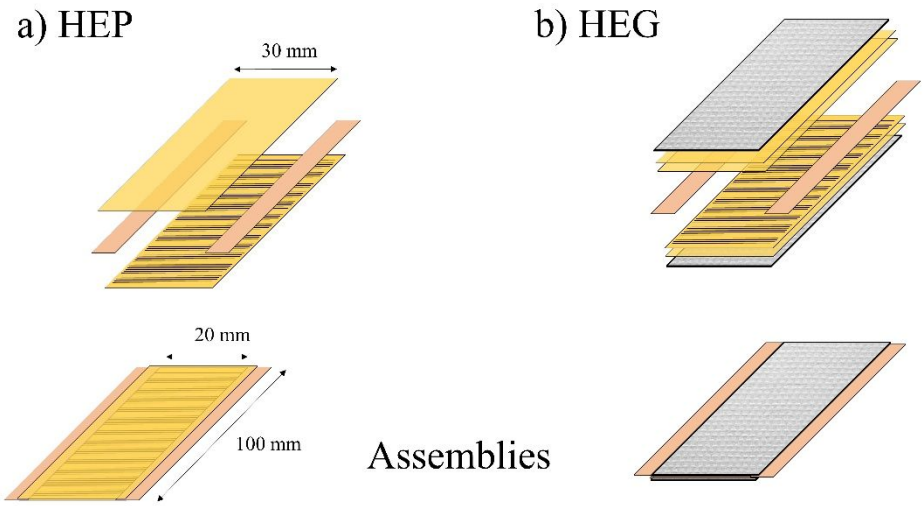

Figure 2 – Exploded view of a) HEP and b) HEG heating elements.

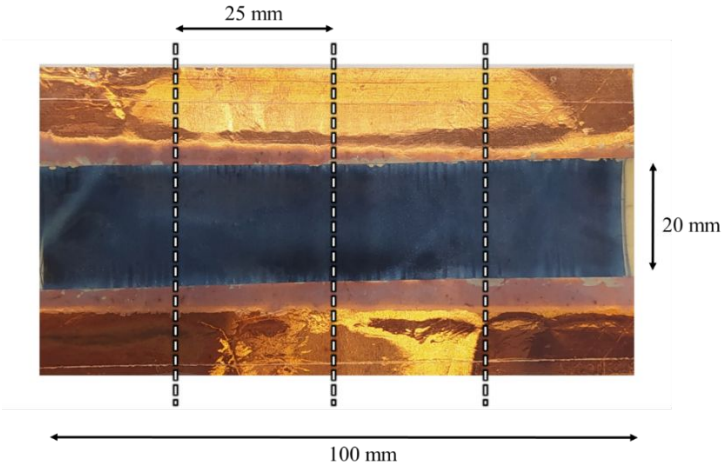

Figure 3 – Picture of a completed heating element (HEP) with sizes and cutting lines.

The test specimens were prepared from two laminates supplied by Solvay:

i) a quasi-isotropic laminate with layup $[45, 90, -45, 0, 45, 0, -45, 90]_S$ made ~~from~~ of PEKK ~~APC-AS4~~ (APC-AS4- areal weight of 145 g/m^2~~gsm~~, resin content of 34%,) with a thickness of 2.24 mm, hereinafter denoted as CF-PEKK;

ii) a laminate made by adding to one face of the previous laminate (i.e. CF-PEKK) an outer ply of plain weave glass fabric (areal weight of 50 g/m^2~~gsm~~) with a thickness of 2.30 mm, hereinafter denoted as CF-PEKK_G.

Both laminates were cut into 100 mm × 25 mm specimens and thoroughly cleaned with *iso*-propyl alcohol to remove grease and dust. For all material systems (i.e. CF-PEKK and CF-PEKK_G†), two specimens were positioned as shown with a 17 mm overlap with a CNT heating element (Fig. 4), taking care not to leave the copper electrode within the overlap of the specimens. For the manufacturing of single lap shear specimens for mechanical tests, ~~The~~ HEP elements were paired with CF-PEKK_G specimens (glass fabric innermost, Fig 4b) while the HEG elements were used with the CF-PEKK specimens (Fig. 4a). This pairing ensures that electrical leakage does not happens between the parts. Kapton film, 50 micrometres thick, was used in the case of CF-PEKK/HEG, to insulate the copper electrodes from the welding parts (Fig. 4a). Each specimen assembly was placed in a frame to maintain correct alignment, the electrodes connected to a power supply through simple clip connection (Fig. 4c) and a pneumatic ram used to apply controlled consolidation pressure. The heating element was energized until welding was achieved and then the assembly allowed to cool in the frame to below 100 °C.

† CF-PEKK_G specimens were placed with the outer layer of glass fibre facing the heating element in order to prevent current leakage.

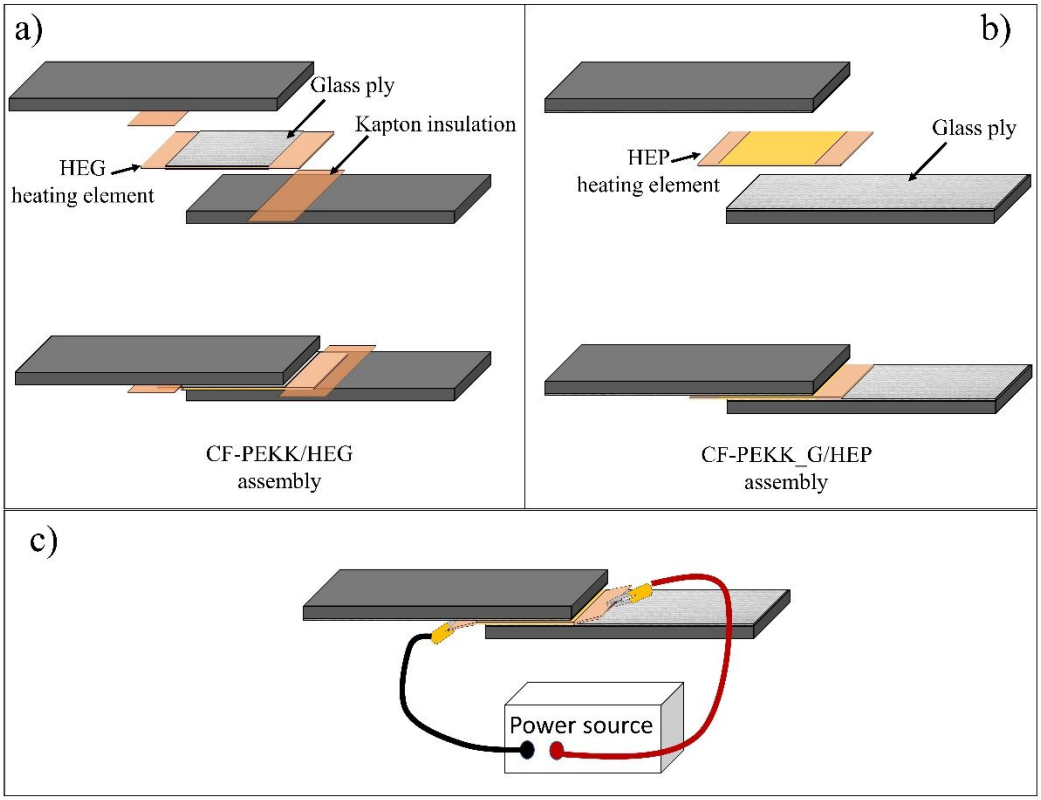

Figure 4 – a) and b) Assembly of welding specimens and heating elements to form a single lap sample for mechanical tests and c) scheme of power supply connection

1.2 Electrical characterization of the heating element

The sheet resistivity, ρ, of the ~~heating element~~single layer of web is:

$$\rho = R^{wN}/l \quad (1)$$

where R is the electrical resistance; $l = 20\text{mm}$ is the distance between the electrodes; $w = 25\text{mm}$ is the width of the insert, and $N = 10$ is the number of CNT-web layers.

The sheet resistivity computed with equation (1), for the single CNT-web layer, ~~-~~does not depend upon the length and~~,~~ width ~~and number of CNT-web layers~~, and allows to estimate the power necessary to melt the interface.

The specific power, W_s, defined as electrical power W per unit area (of the heating element), can be calculated as:

$$W_s = \frac{I^2 R}{lw} = \frac{I^2 \rho}{Nw^2} \quad (2)$$

where I is the electrical current, maintained constant throughout the welding process in this study. It is worth noting that if the resistivity of the heating element is measured at room temperature,ρ_0, the use of equation (2) is not rigorous at high temperatures since the resistivity itself depends on the temperature.

Preliminary experiments conducted at temperatures between 20 and 350°C (slightly above the melting point of PEKK) have shown that the resistivity of the heating element decreases linearly with the temperature (Fig. 5). Consequently, also the specific powerW_s applied during the welding process changes linearly with the temperature of the CNT web.

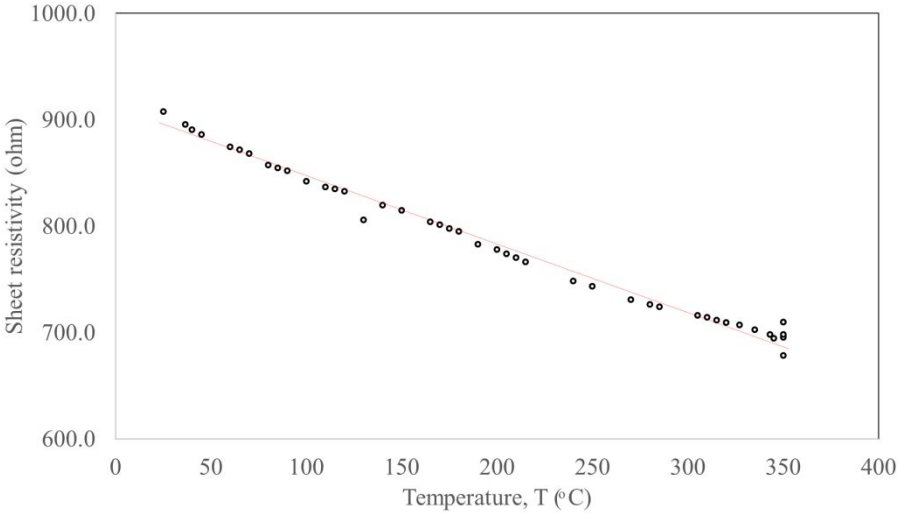

Figure 5 – Heating element sheet resistivity change under different temperatures.

It should be noted that different CNT forests can have different electrical properties depending upon CNT length, CNT number of walls, diameter and web density [40]. Moreover, the electrical properties can be affected by various anomalies of the network such as structural flaws, nanotube misalignment or poor densification. As an example, figure 6 shows, for two different batches of CNT forest, the values of the sheet resistivity measured on 56 and 97 heating elements produced using two different batches of CNT forest.

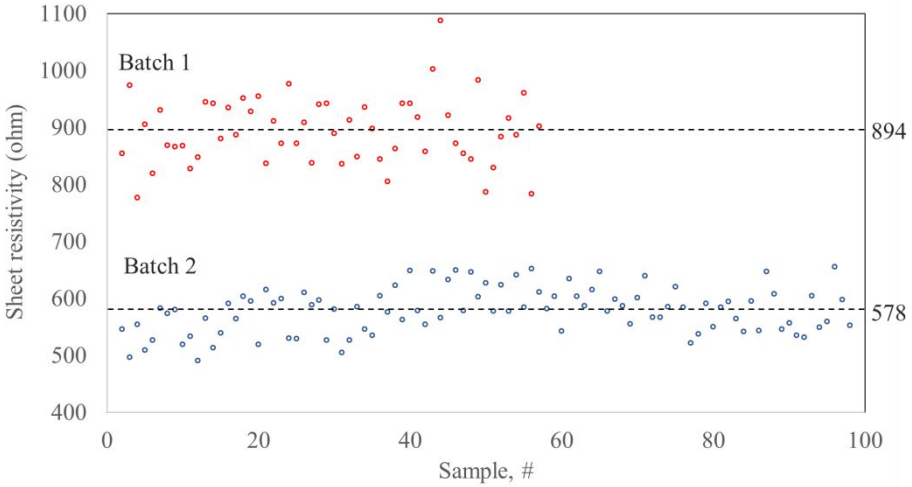

Figure 6 – Sheet resistivity values at room temperature measured on heating elements produced using two different CNT forest batches.

It can be seen that batch 1 has an average sheet resistivity (mean value = 894 Ω, SDV=59.2 Ω) which is 55% larger than that of batch 2 (mean value = 578 Ω, SDV=39.8 Ω).

1.3 Thermal characterization of the heating element

The heating element transfers heat to the substrate through conduction and, in the exposed regions of the heating element that lie outside the sample overlap (Fig.7), to the surrounding environment through convection and irradiation. Since radiation and convection represent, for the case under investigation, less efficient ways of heat transfer, the temperature of the exposed regions is usually much higher than that within the overlap. This leads to higher temperatures at the entry point (Fig. 7) that could potentially cause polymer degradation and heater failure in the vicinity of the edges.

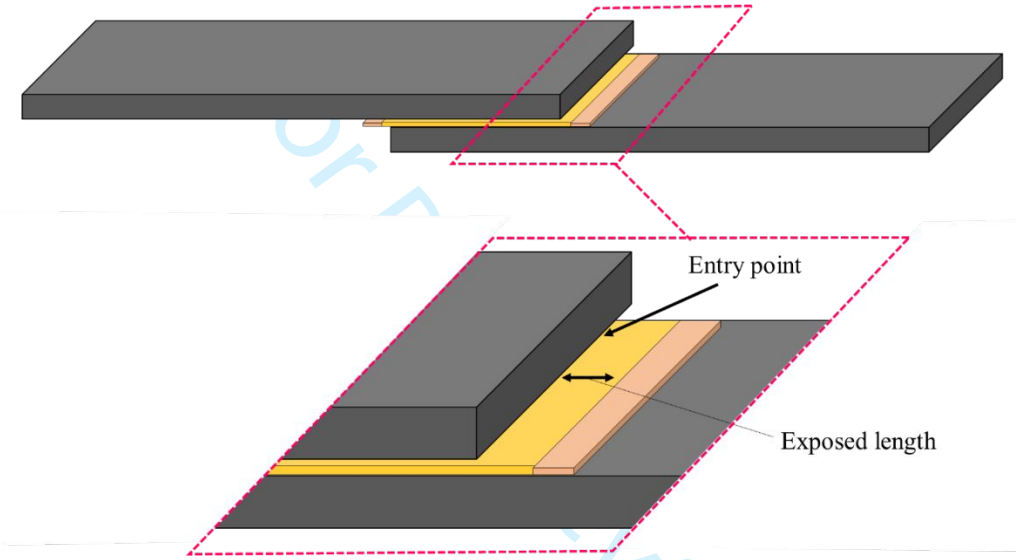

Figure 7 – Exposed length of heating element and detail of the penetration area.

This is a well-known problem with traditional heating elements (metallic meshes or carbon fibre) that need to be clamped to minimise the contact resistance between the electrode and the heating element and that necessarily have a large exposed area.

CNT web heating elements, on the contrary, were fabricated by directly connecting the copper electrodes, necessary to deliver the power, at the edges of the CNT web. With this technique, the area of the exposed region is minimized, and the mass and thermal conductivity of the copper buses is considerably higher than that of the adjacent web and this leads to a much more uniform temperature distribution within the electrodes.

A thermographic image of a strip of heating elements (i.e. prior to subdivision) brought to an average temperature of ~80 °C (Fig. 8) reveals that the temperature over the body of the heating elements (averaged over the areas represented in Fig~~fig~~. 8) is virtually uniform and that it decreases abruptly in the vicinity of the

electrodes. This means that with the technique used to manufacture the heating elements, the resistance at the contact point between the CNT-webs and the electrode is lower than the resistance within the CNT-web itself, and confirms that no clamping is needed to reduce the contact resistance, thus simplifying the welding process.

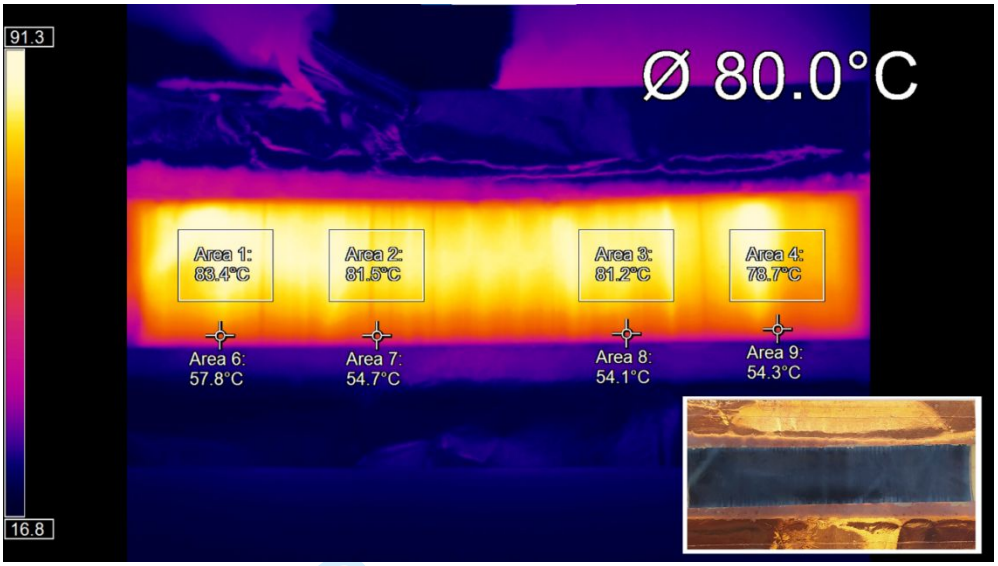

Figure 8 – Thermal image of a heating element (HEP type) (20 mm x 100 mm) brought at an average temperature of 80 °C and temperature measurement at different locations.

1.4 Welding process and related parameters

1.4.1 Power delivery

The welding process can be performed mainly by either using constant voltage [19,21] or constant current supply [2,24,34] although different approaches (i.e. ramped voltage application) can be used [28].

Since the sheet resistivity and hence heating element resistance decreases linearly with the temperature, application of a constant voltage results in an increase in the current and hence an increase in power. However, a sudden and drastic decrease in the resistance (due for example to current leakage) will cause a substantial increase in the power and could lead to a localized runaway and risk of burning or fire. Conversely, an increase in the resistance (caused for example by a small break in the CNT web) will cause the delivered current, and thus the power, to decrease substantially. Hence, the welding could fail because of the insufficient energy delivered.

Contrarily, at constant current, which is achieved by automatically varying the voltage, the power will decrease in line with the resistivity as the temperature rises, thereby slowing the temperature rise and extending the time required. However, if the resistance drops drastically because of current leakage, the power will drop as well (Fig. 9~~11~~) making the welding process much safer. Moreover, an increase in the resistance, due for

example to a local rupture of the web, will cause the power, and therefore, the temperature to increase (Fig. 9) but only up to a safe voltage limit, making the welding more likely to succeed. For the aforementioned reasons, all welding experiments reported here were run at constant current.

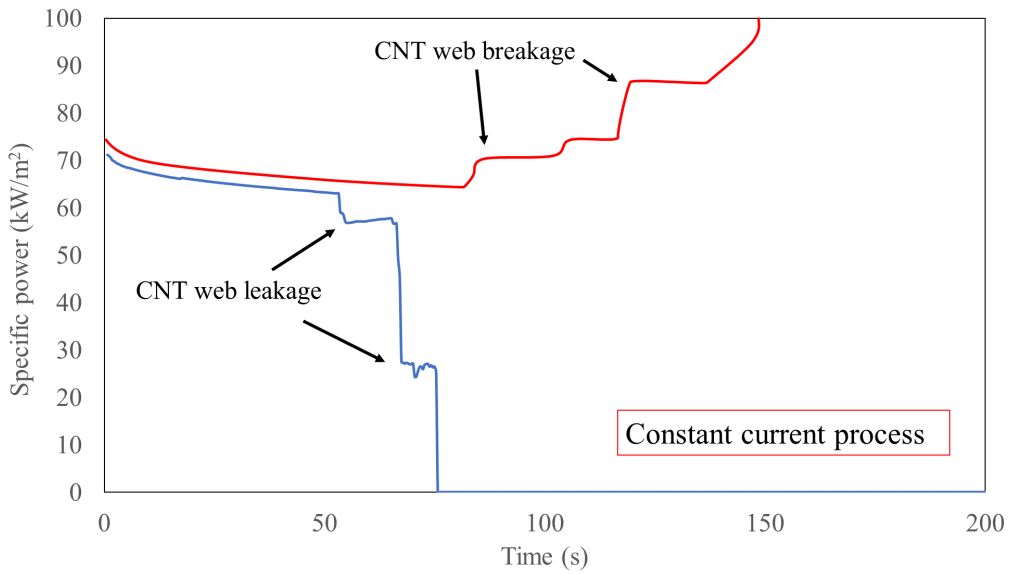

Figure 9 – Characteristic electrical profiles of heating elements experiencing CNT web breakage or leakage under a constant current supply.

1.4.2 Pressure control

The consolidation pressure plays a major role in polymer welding because it promotes polymer interdiffusion and ensures that small gaps, due to manufacturing imperfections, curvature, or specific manufactured features, are brought together and the whole of the weld interface is in contact. When joining large parts, high consolidation pressure is problematic because it requires robust and expensive tooling. The lowest effective consolidation pressure for the proposed technology is therefore identified and used in experiments to best inform its use in an industrial environment. Preliminary experiments found that the lowest consolidation pressure for which the mechanical behaviour of the joint is satisfactory and repeatable is 0.05 MPa, and is thus used in all the experiments.

1.4.3 Time and power control

After fixing the consolidation pressure, the two major parameters investigated are the welding time t (at three levels: 60, 105, 150 s), and the initial specific power W_{s0} supplied to the heating element (also at three levels: 70, 80, 90 kW/m²). The initial specific power $W_{s0} = I^2\rho_0/Nw^2$ is calculated with equation (2) using the sheet resistivity measured at room temperature, ρ_0.

1.5 Leakage effect in CF-PEKK

Welding of conductive composites can be drastically affected by electrical leakage during which electrical current finds an alternative, significantly lower resistance, path than through the heating element, thereby preventing parts of the element from reaching the desired temperature, and generating local hot spots at the contact points. To investigate current leakage, a HEP heating element was sandwiched between CF-PEKK specimens and, after applying pressure, provided with a constant current. With no glass fabric insulation layer, direct contact between the CNT web in the heating element and the carbon fibre of the substrates can occur. Depending upon how quickly and severely the leak develops, the weld may not succeed at all or may fail at substantially lower loading. The fracture surface of the failed test sample (Fig. 10) shows an area of unwelded interface surrounding a small contact point.

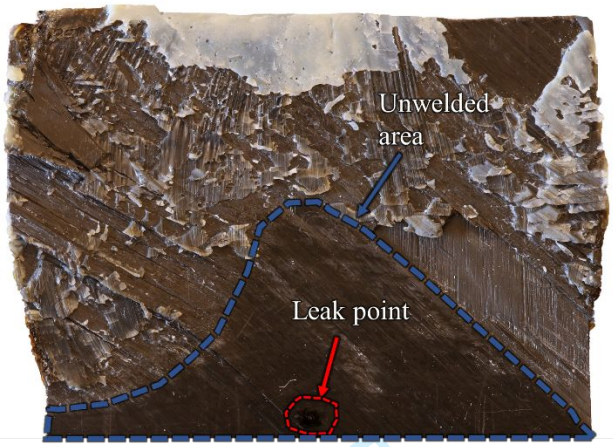

Figure 10 – Surface of a welding sample affected by current leakage and characterized by a leaking point and an unwelded area.

During the welding process, the leakage event can be detected by monitoring the current, voltage and power being applied. As the sample is otherwise electrically isolated, leakage requires two points of electrical contact between the substrate and CNT web. In our study three main types of contact locations were identified: i) the front-edge, ii) the side-edge and iii) point contacts on the mating surface (Fig. 11).

Figure 11 shows three examples of:

1) Point to point path (Fig~~fig~~. 11a), where current leaks between local point contacts;
2) Point to front-edge path (Fig~~fig~~. 11b), where the current leaks from a local point contact to a front edge contact adjacent to a copper bus;
3) Side-edge to Side-edge (~~fig~~Fig. 11c), where the current propagates from one side to the other of the substrate.

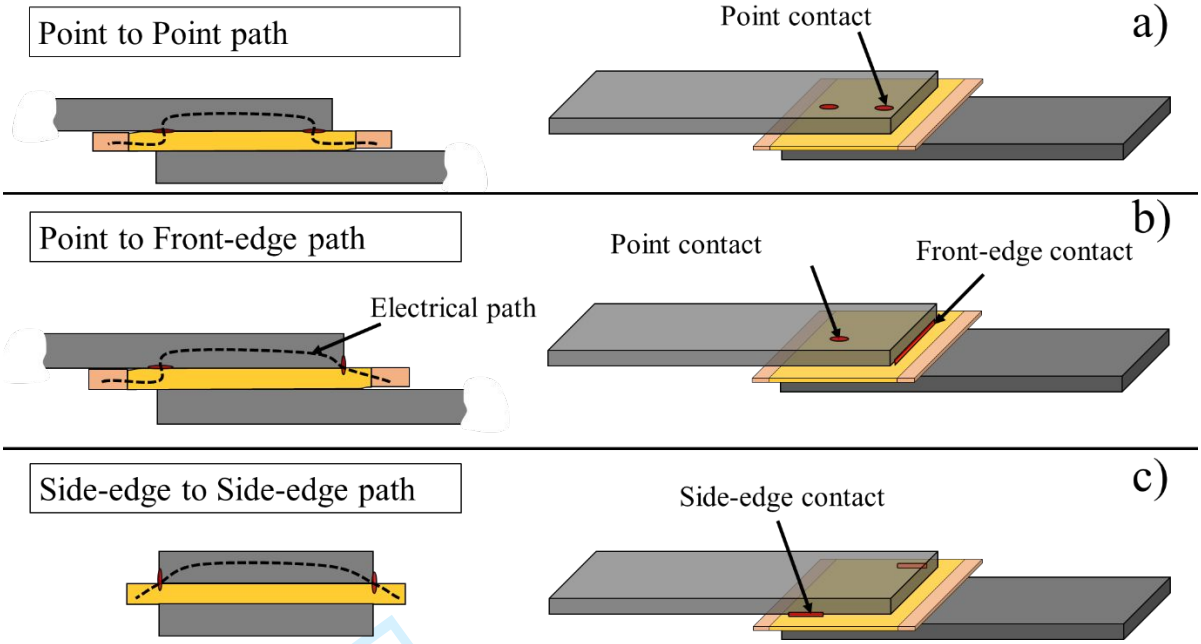

Figure 11 – Illustration of the three main types of contact and the possible current path: a) Electrical current moving from one point contact to another, b) current moving from a point contact to a front-edge contact and c) current moving from one side-edge contact to another.

In our study, the third type of current leakage, the side-edge to side-edge, was mainly avoided by cutting the heating elements slightly smaller than the welding parts in a way that the sides contacts between the heating element and the composite parts were fully avoided.

However, this method does not prevent current leakage from the other locations and, for this reason, different methods were investigated to reduce the event:

1. Increase the thickness of the polymer film enclosing the heating element.
2. Include a robust (e.g. glass fabric) insulating layer between the heating element and the substrate.

1.5.1 Polymer film insulation

HEP heating elements were used alone or embedded within additional films of PEKK (denoted as HEP+1L and HEP+2L if 1 or 2 additional layers per side are used, respectively), to determine if the addition of polymer can prevent electrical leakage at the specific powers of 70 kW/m^2 or 90kW/m^2. The as-prepared HEP element does not prevent current leakage at 70 kW/m^2 (Fig.12a) but the addition of one extra layer of polymer (i.e. HEP+1L) is sufficient to allow successful welding. On the other hand, if a higher power is used (90 kW/m^2) (Fig. 12b) neither HEP+1L nor HEP+2L will guarantee insulation between the parts. At the higher power, the polymer film presumably melts more quickly and to a higher temperature before the interfaces have softened sufficiently to bond. The applied pressure, in combination with the lower viscosity of the melted polymer film, increase the probability of creating an electrical contact with the substrates [4,21].

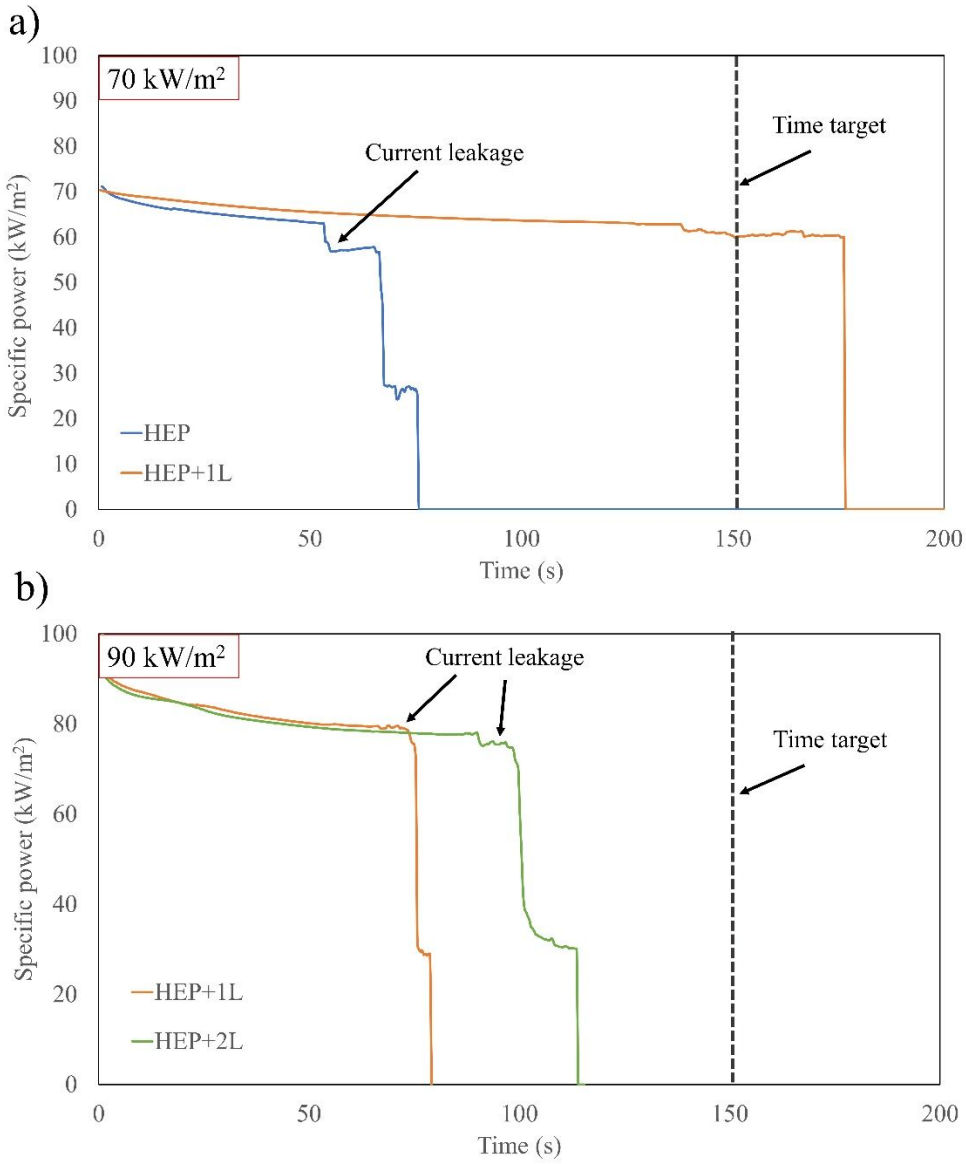

Figure 12 – Electrical profile of welding processes carried at: a) 70 kW/m², using heating elements HEP and HEP+1L, and b) at 90 kW/m² using heating elements HEP+1L and HEP+2L.

1.5.2 Glass fabric insulation

HEG heating elements were used to weld CF-PEKK substrates using an initial specific power of 80 kW/m². Ten samples of each type were produced and it was found that in 80% of cases, welding was completed (to the time target of 150 seconds) without current leakage in samples welded using the 25 g/m²~~gsm~~ ply. Samples welded with the 50 g/m²~~gsm~~ glass ply were successfully joined in 100% of cases (Fig. 13). The failure of the 25 g/m²~~gsm~~ glass ply in 20% of cases is attributed to the presence of random gaps that can be found in the glass fabric.

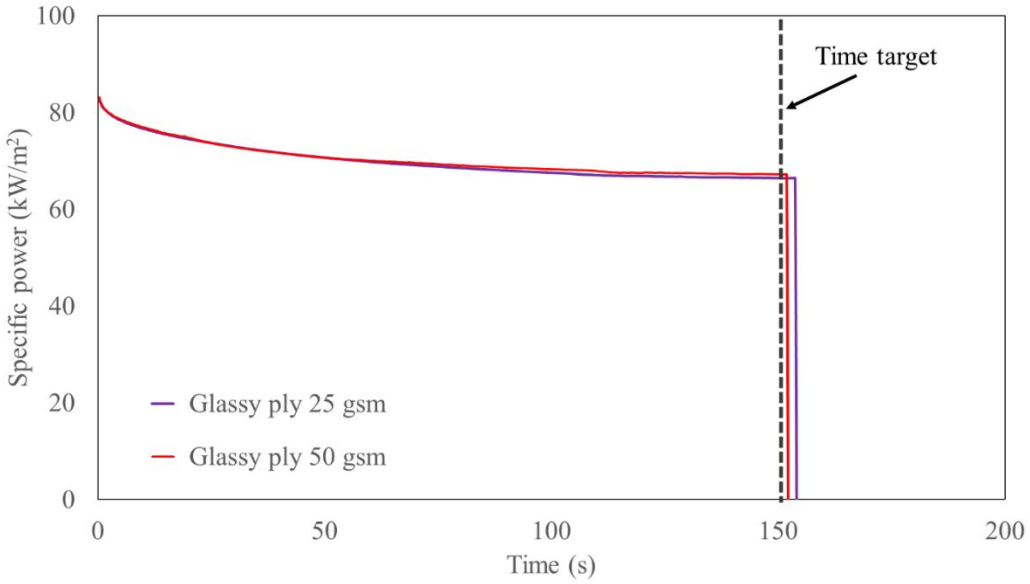

Figure 13 – Electrical profile of welding processes carried out at 80 kW/m² for 150 seconds using heating element insulated by using glass fibre ply (heating element of type 2).

1.6 Mechanical tests and fractographic analyses

Single lap shear specimens were tested using a Zwick Roell z100 universal testing machine equipped with a 100 kN load cell. ~~and tests were performed following the ASTM D5868~~. A loading speed of 1 mm/min was used for all the specimens.

The shear strength of the samples was calculated as $\tau = P/A$, where P is the peak load measured during the test and A is the nominal area of the sample overlap. Notice that this does not necessarily equal the effective welded area which might be smaller in case the ligament has not been entirely melted. The fracture surface of samples was then observed using a Canon EOS 80D camera and Canon EF 100 mm f/2.8L Macro IS USM lens and different types of fractures were reported accordingly to the definitios of ASTM D5868 standard.

2 Results and discussion

2.1 CF-PEKK_G/HEP samples

2.1.1 Experimental results

Samples welded at the two highest powers and the longest time (150s) show the highest mechanical performances with values close to 30 MPa (Fig. 14). On the contrary, samples welded for only 60 seconds show the lowest mechanical performance with values under 4 MPa for the highest power, or complete failure for the lower power/time combinations. Furthermore, samples welded for 150s or using the two highest specific powers show a welded area above 85% with the highest value of 100% welded area for samples welded at the higher power/time combination (Tab. 1).

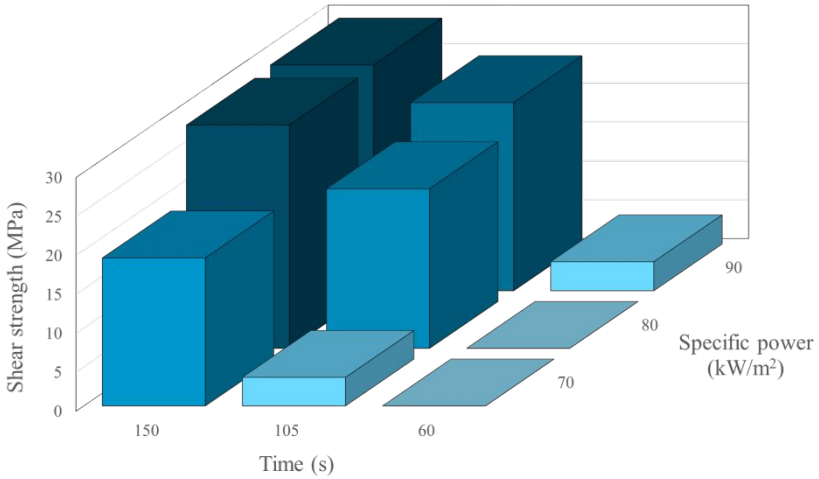

Figure 14 – Shear strength of welded (CF-PEKK_G/HEP) at different Specific power and Time.

Table 1 – Welded area and single lap shear test statistics for welded (CF-PEKK_G/HEP) at different Specific power and Time.

Factors		Single lap shear test results		Statistic characteristic		
Specific power (kW/m²)	**Time (s)**	**Welded area (%)**	**Shear strength (MPa)**	**Average (MPa)**	**St. Dev (MPa)**	**CV (%)**
90	150	100 100 100	27.3 28.4 31.3	29.0	2.07	7.1
90	60	13 20 33	2.5 4 4.7	3.7	1.12	30.1
70	60	0 0 0	N.A. N.A. N.A.	N.A.	N.A.	N.A.
70	150	79 81 85	17.7 20.2 19.1	19.0	1.25	6.6
80	105	77 100 85	19.7 20.3 21.5	20.5	0.92	4.5
70	105	23 18 21	4 3 4	3.7	0.58	15.7
80	150	100 100 100	28.1 29.4 28.5	28.7	0.67	2.3
80	60	0 0 0	N.A. N.A. N.A.	N.A.	N.A.	N.A.
90	105	98 100 100	22.3 26.2 24	24.2	1.96	8.1

2.1.2 Heat affected zone (HAZ) of the joints

In any welding process, a zone is created adjacent to the bond in which the material is affected by the heat flux although not necessarily melted. Insofar as the thermal effect is likely to be neutral or negative rather than positive, it is important to keep this heat affected zone (HAZ) as narrow as possible. In the present work, ~~plastic~~ thermal deformation of the joint plies as indicated by edge splitting and crushing are taken as a proxy indication of HAZ thickness. The affected thickness is 50 to 100% for the joints welded at 90 kW/m^2, around 20 to 50% for 80 kW/m^2 and zero to about 10% 70 kW/m^2 (Fig. 15). A good compromise of welding reliability, strength and HAZ minimization is obtained powering the heating element at 80 kW/m^2 for 150 seconds.

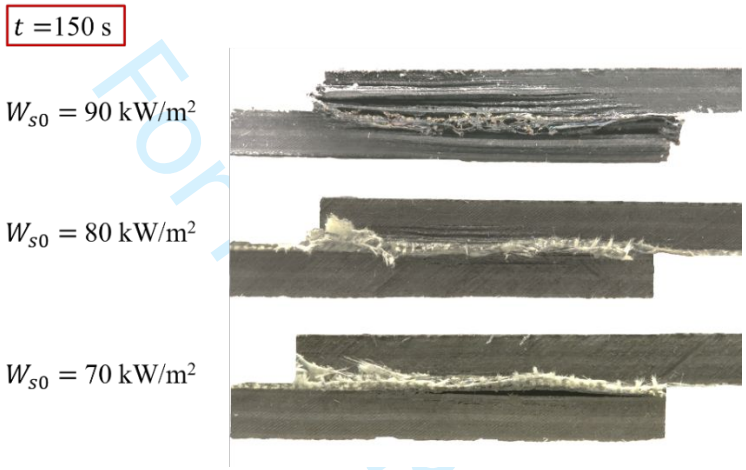

Figure 15 – Plastic deformation of welded CF-PEKK_G/HEP samples welded for 150 seconds and with a specific power equal to 90 kW/m^2, 80 kW/m^2 and 70 kW/m^2 respectively.

2.1.3 Processing window

The processing window (Fig.16) was generated by plotting the values of shear strength, obtained at the different points of the experimental space, against the two factors, specific power and time. Some additional samples were prepared, at 100 kW/m^2 applied power for 60 and 105 seconds, and tested to clarify the general limits of the acceptable processing area.

The light grey area (Fig. 16) indicates a condition of under-welding. Under this condition, the average portion of the joint area successfully welded was below 85%.

Samples with a welded area above 85% fall within the mid-grey 'fully welded' zone and are characterized by the higher mechanical performance obtained. Although having 100% weld area and of high strength, samples falling within the dark grey area are considered to be 'over welded', having a HAZ greater than 50%. The optimum processing window is located between the welding times of 105 and 150 seconds with the highest mechanical performances in correspondence of 80 and 90 kW/m^2 and 150 seconds. It is worth noting that the processing window area, generated after 150 seconds, was created solely by analysing the HAZ of the samples.

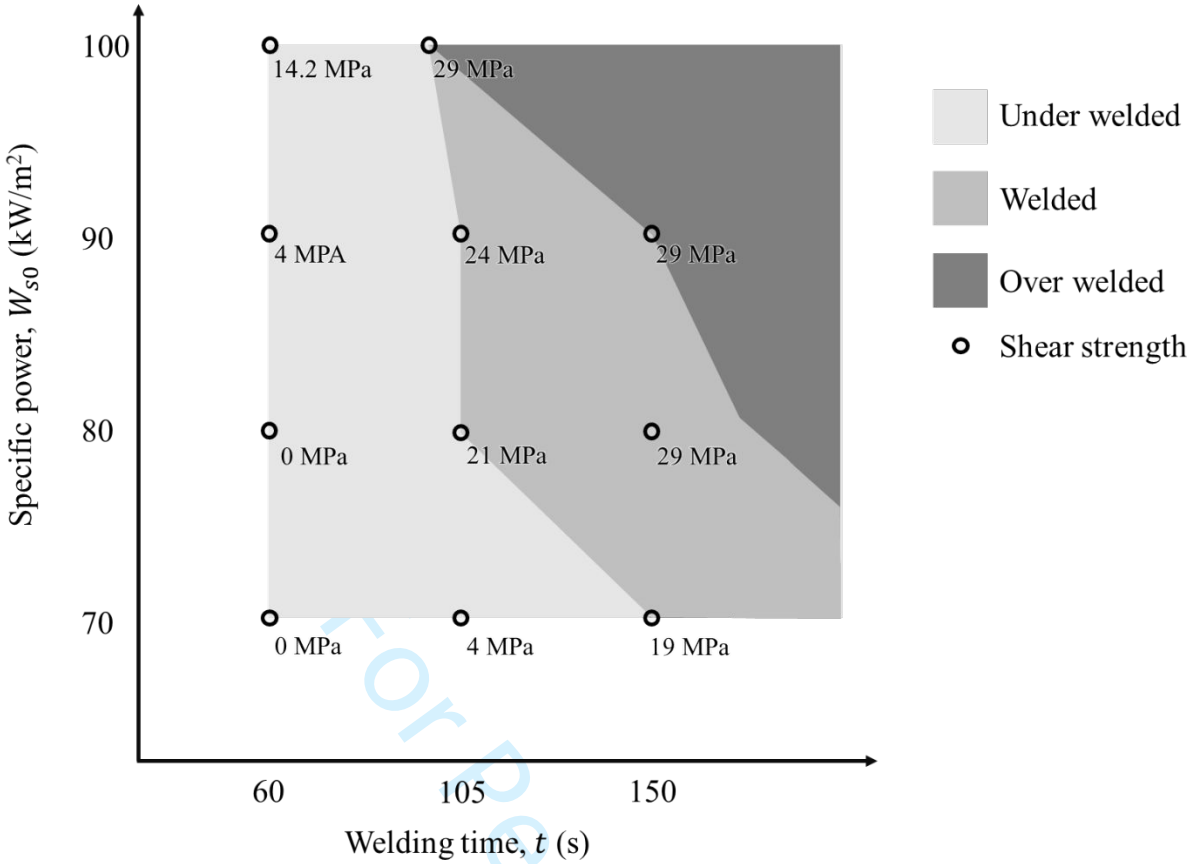

Figure 16 – Processing window for the welding of CF-PEKK_G/HEP samples with reported values of shear strength.

2.1.4 Analysis of fracture surface

Three types of failure can be detected in the broken samples:

i) Intrainsert failure (Fig. 17a), when the crack propagates within the heating element. This type of fracture is caused either by the polymer film failing to fully penetrate the CNT web structure, either because the web is too thick or dense, too little pressure, time or heat is applied, or air has become trapped in the structure; or by the element degrading during use. The element is necessarily hotter than required to melt the polymer in order to create a temperature gradient steep enough to join the components in a reasonable time. The key constraint on further increasing the power and hence temperature is the thermal degradation caused to the polymer of the element before welding is completed.

ii) Adhesive failure (Fig. 17b), when the crack propagates between the heating element and substrate. This type of failure occurs when the polymer interdiffusion does not (completely) happen. This is caused by process variables of insufficient time and/or power and/or pressure. Otherwise, current leakage can rob the surrounding area of the energy to heat sufficiently.

iii) Fibre-tear failure (Fig.17c), where the crack propagates in the substrate and fibre plies (deep fibre-tear failure) or matrix with a few fibres (light fibre-tear failure) of the substrate is transferred to the heating element surface, is usually related to a good welding performance. In the present work, it was observed with successful welds that cracks propagated deep into the substrate, breaking one or multiple plies of carbon fibre. If, in small portions, the crack also propagates into and through the heating element, or between the heating element and substrate with little or no diminution of strength, this would also be considered to be fibre-tear failure.

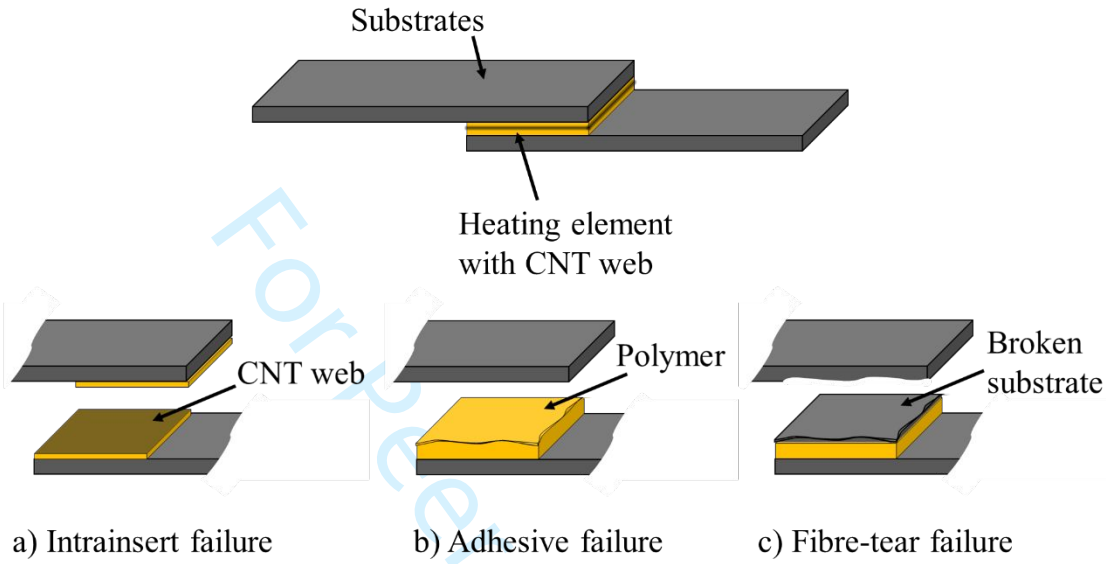

Figure 17 – Main types of detected failures in welded samples after single lap shear test.

Figure 18 reports a comparison of the fracture surface for specimens welded with a specific power W_{s0}= 90 kW/m^2, 80 kW/m^2 and 70 kW/m^2. All specimens were welded using a welding time of 150 seconds and consolidation pressure of 0.05 MPa. Samples welded using 90 and 80 kW/m^2 show fibre-tear type of failure, however, samples welded at 90kW/m^2 show a larger area of deep fibre-tear failure compared to specimens welded at 80 kW/m^2. The additional amount of provided energy, compared to samples welded with lower power, results in an improved bond between the substrates and the heating element. This is also confirmed by the fact that samples welded with the 70kW/m^2 not only do not present a deep fibre-tear type of failure but show portions of adhesive failure (Figfig. 18c) with a consequent lower strength.

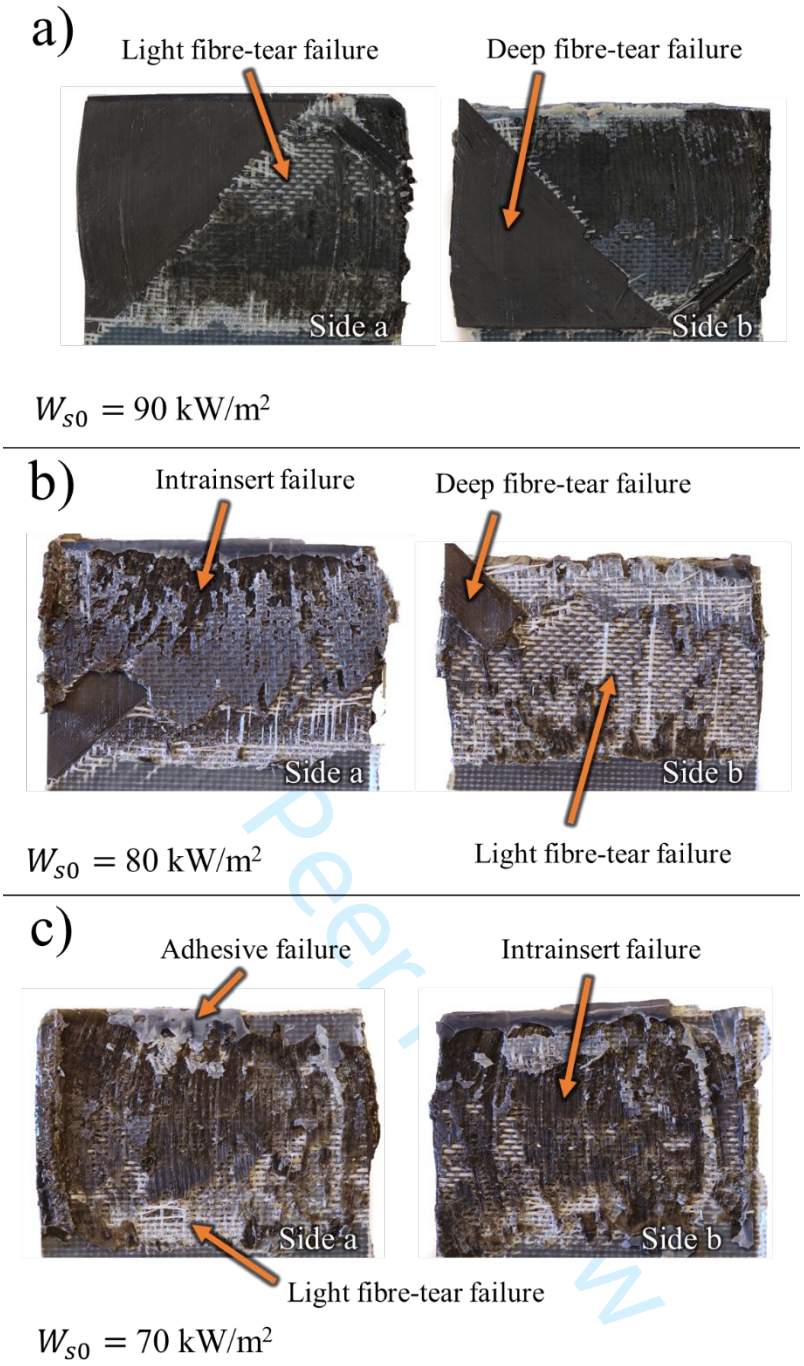

Figure 18 – Failure surface of single-lap shear test CF-PEKK_G/HEP samples welded for 150 seconds and with a specific power equal to a) 90 kW/m², b) 80 kW/m² and c) 70 kW/m² respectively.

2.2 CF-PEKK/HEG samples

As a concept demonstration, substrates of CF-PEKK were welded using the pre-made HEG heating elements having the 50 g/m²~~gsm~~ glass ply on each face to prevent current leakage. This configuration is helpful to simplify the manufacturing process of thermoplastic composites by eliminating the need to include a ply of glass fabric in their original configuration. Three samples were welded at pressure p= 0.05 MPa, using the best welding parameter found when welding CF-PEKK_G/HEP (i.e. 80 kW/m² and 150 s).

Table 4 - Results for single lap shear test of CF-PEKK/HEG at different specific power and time

Factors		Single lap shear test results		Statistic characteristic		
Power (kW/m²)	Time (s)	Welded area (%)	Response (MPa)	Average (MPa)	St. Dev (MPa)	CV (%)
80	150	100	26.02	25	1.28	5.12
		100	25.50			
		100	23.58			

The single-lap shear test produced a mean shear strength of 25 MPa which is slightly lower than the value reported for CF-PEKK_G/HEP for the same welding parameters. This difference is possibly attributable to a slight difference in thermal conductivity across the glass-carbon fibre interface compared with the polymer-glass interface of the CF-PEKK_G/HEP construction, perhaps influenced by the element or substrate topography. Further optimisation of the process would clarify and eliminate this difference.

3 Conclusion

The following concluding remarks can be made:

- The heating elements are extremely flexible and can be easily conformed to any shape. They exhibit uniform temperature and resistivity that decreases linearly with the applied temperature.
- Single lap shear specimens CF-PEKKG/HEP have shown a shear strength of 30 MPa. This was obtained applying a consolidation pressure of 0.05 MPa, an initial specific power of 80-90 kW/m² for a period of time of 150 s.
- The optimum processing window, which take into consideration mechanical performance and thermal deformation of the components, was found to be located between the welding times of 105 and 150 seconds.
- Single lap shear specimens CF-PEKK/HEG have shown a slightly lower shear strength, 25 MPa, using the same processing parameters.
- Post-mortem analyses showed that optimum specimens exhibited a fibre-tear failure with a crack propagating within the substrate.
- The results obtained demonstrate the potential of the proposed welding technology and suggest the prospect to use it in an industrial environment.
-

Acknowledgements

This work was supported by the project SPaRK which has received funding from the European Union's Horizon 2020 research and innovation programme under the Marie Sklodowska-Curie grant [grant agreement No 754507].

Acknowledgements

The raw/processed data required to reproduce these findings cannot be shared at this time due to technical or time limitations.

References

[1] C. Ageorges, L. Ye, M. Hou, Advances in fusion bonding techniques for joining thermoplastic matrix composites: a review, Compos. Part A Appl. Sci. Manuf. 32 (2001) 839–857. https://doi.org/10.1016/S1359-835X(00)00166-4.

[2] C. Ageorges, Experimental investigation of the resistance welding of thermoplastic-matrix composites. Part II: optimum processing window and mechanical performance, Compos. Sci. Technol. 60 (2000) 1191–1202. https://doi.org/10.1016/S0266-3538(00)00025-7.

[3] C. Ageorges, L. Ye, Resistance Welding of Metal/Thermoplastic Composite Joints, J. Thermoplast. Compos. Mater. 14 (2001) 449–475. https://doi.org/10.1106/PN74-QXKH-7XBE-XKF5.

[4] C. Ageorges, L. Ye, M. Hou, Experimental investigation of the resistance welding for thermoplastic-matrix composites. Part I: heating element and heat transfer, Compos. Sci. Technol. 60 (2000) 1027–1039. https://doi.org/10.1016/S0266-3538(00)00005-1.

[5] C. Ageorges, L. Ye, Y.W. Mai, M. Hou, Characteristics of resistance welding of lap shear coupons. Part II. Consolidation, Compos. Part A Appl. Sci. Manuf. 29 (1998) 911–919. https://doi.org/10.1016/S1359-835X(98)00023-2.

[6] E.C. Eveno, J.W. Gillespie, Resistance Welding of Graphite Polyetheretherketone Composites: An Experimental Investigation, J. Thermoplast. Compos. Mater. 1 (1988) 322–338. https://doi.org/10.1177/089270578800100402.

[7] A. Yousefpour, M. Hojjati, J.-P. Immarigeon, Fusion Bonding/Welding of Thermoplastic Composites, J. Thermoplast. Compos. Mater. 17 (2004) 303–341. https://doi.org/10.1177/0892705704045187.

[8] X. Xiong, D. Wang, J. Wei, P. Zhao, R. Ren, J. Dong, X. Cui, Resistance welding technology of fiber reinforced polymer composites: a review, J. Adhes. Sci. Technol. 35 (2021) 1593–1619. https://doi.org/10.1080/01694243.2020.1856514.

[9] K.C. Warren, R.A. Lopez-Anido, A.L. Freund, H.J. Dagher, Resistance welding of glass fiber reinforced PET: Effect of weld pressure and heating element geometry, (n.d.). https://doi.org/10.1177/0731684416633516.

[10] D. Stavrov, H.E.N.N. Bersee, Resistance welding of thermoplastic composites-an overview, Compos. Part A Appl. Sci. Manuf. 36 (2005) 39–54. https://doi.org/10.1016/j.compositesa.2004.06.030.

[11] H. Shi, I.F. Villegas, H.E.N. Bersee, A displacement-detection based approach for process monitoring and processing window definition of resistance welding of thermoplastic composites, Compos. Part A Appl. Sci. Manuf. 74 (2015) 1–9. https://doi.org/10.1016/j.compositesa.2015.03.002.

[12] H. Shi, I.F. Villegas, H.E.N. Bersee, Strength and failure modes in resistance welded thermoplastic composite joints: Effect of fibre–matrix adhesion and fibre orientation, Compos. Part A Appl. Sci.

Manuf. 55 (2013) 1–10. https://doi.org/10.1016/j.compositesa.2013.08.008.

[13] V. Rohart, L.L. Lebel, M. Dubé, Effects of environmental conditions on the lap shear strength of resistance-welded carbon fibre/thermoplastic composite joints, Compos. Part B Eng. 198 (2020) 108239. https://doi.org/10.1016/j.compositesb.2020.108239.

[14] V. Rohart, L.L. Lebel, M. Dubé, Influence of freeze/thaw cycling on the mechanical performance of resistance-welded carbon fibre/polyphenylene sulphide composite joints, J. Reinf. Plast. Compos. 39 (2020) 837–851. https://doi.org/10.1177/0731684420933681.

[15] J.P. Reis, M. de Moura, S. Samborski, Thermoplastic Composites and Their Promising Applications in Joining and Repair Composites Structures: A Review, Materials (Basel). 13 (2020) 5832. https://doi.org/10.3390/ma13245832.

[16] X. Li, T. Zhang, S. Li, H. Liu, Y. Zhao, K. Wang, The effect of cooling rate on resistance-welded CF/PEEK joints, J. Mater. Res. Technol. 12 (2021) 53–62. https://doi.org/10.1016/J.JMRT.2021.02.071.

[17] N. Koutras, I.F. Villegas, R. Benedictus, Influence of temperature on the strength of resistance welded glass fibre reinforced PPS joints, Compos. Part A Appl. Sci. Manuf. 105 (2018) 57–67. https://doi.org/10.1016/j.compositesa.2017.11.003.

[18] I. Fernandez Villegas, L. Moser, A. Yousefpour, P. Mitschang, H.E. Bersee, I.F. Villegas, L. Moser, A. Yousefpour, P. Mitschang, H.E. Bersee, Process and performance evaluation of ultrasonic, induction and resistance welding of advanced thermoplastic composites, J. Thermoplast. Compos. Mater. 26 (2013) 1007–1024. https://doi.org/10.1177/0892705712456031.

[19] M. Dubé, P. Hubert, A. Yousefpour, J. Denault, Resistance welding of thermoplastic composites skin/stringer joints, Compos. Part A Appl. Sci. Manuf. 38 (2007) 2541–2552. https://doi.org/10.1016/j.compositesa.2007.07.014.

[20] C. Ageorges, L. Ye, Y.-W. Mai, M. Hou, Characteristics of resistance welding of lap shear coupons. Part I: Heat transfer, Compos. Part A Appl. Sci. Manuf. 29 (1998) 899–909. https://doi.org/10.1016/S1359-835X(98)00022-0.

[21] M. Dubé, P. Hubert, A. Yousefpour, J. Denault, Current leakage prevention in resistance welding of carbon fibre reinforced thermoplastics, Compos. Sci. Technol. 68 (2008) 1579–1587. https://doi.org/10.1016/j.compscitech.2007.09.008.

[22] M. Hou, M. Yang, A. Beehag, Y.-W. Mai, L. Ye, Resistance welding of carbon fibre reinforced thermoplastic composite using alternative heating element, Compos. Struct. 47 (1999) 667–672. https://doi.org/10.1016/S0263-8223(00)00047-7.

[23] S.H. McKnight, S.T. Holmes, J.W. Gillespie, C.L.T. Lambing, J.M. Marinelli, Scaling issues in resistance-welded thermoplastic composite joints, Adv. Polym. Technol. 16 (1997) 279–295. https://doi.org/10.1002/(SICI)1098-2329(199711)16:4<279::AID-ADV3>3.0.CO;2-S.

[24] L.C.M. Barbosa, S.D.B. de Souza, E.C. Botelho, G.M. Cândido, M.C. Rezende, Fractographic study of

welded joints of carbon fiber/PPS composites tested in lap shear, Eng. Fail. Anal. 93 (2018) 172–182. https://doi.org/10.1016/j.engfailanal.2018.07.007.

[25] M. Hou, L. Ye, Y.W. Mai, An Experimental Study of Resistance Welding of Carbon Fibre Fabric Reinforced Polyetherimide (CF Fabric/PEI) Composite Material, Appl. Compos. Mater. 6 (1999) 35–49. https://doi.org/https://doi.org/10.1023/A:1008879402267.

[26] M. Dubé, P. Hubert, J.N.A.H. Gallet, D. Stavrov, H.E.N. Bersee, A. Yousefpour, Fatigue performance characterisation of resistance-welded thermoplastic composites, Compos. Sci. Technol. 68 (2008) 1759–1765. https://doi.org/10.1016/j.compscitech.2008.02.012.

[27] D. Brassard, M. Dubé, J.R. Tavares, Resistance welding of thermoplastic composites with a nanocomposite heating element, Compos. Part B Eng. 165 (2019) 779–784. https://doi.org/10.1016/j.compositesb.2019.02.038.

[28] M. Dubé, P. Hubert, J.N. Gallet, D. Stavrov, H.E. Bersee, A. Yousefpour, Metal mesh heating element size effect in resistance welding of thermoplastic composites, J. Compos. Mater. 46 (2012) 911–919. https://doi.org/10.1177/0021998311412986.

[29] X. Xiong, D. Wang, J. Wei, P. Zhao, R. Ren, J. Dong, L. Tian, W. Wang, C. Xu, Resistance welding of thermoplastics by carbon nanotube-grafted heating element, J. Adhes. Sci. Technol. 35 (2021) 1806–1819. https://doi.org/10.1080/01694243.2020.1860564.

[30] I.F. Villegas, H.E.N. Bersee, Characterisation of a metal mesh heating element for closed-loop resistance welding of thermoplastic composites, J. Thermoplast. Compos. Mater. 28 (2015) 46–65. https://doi.org/10.1177/0892705712475012.

[31] X. Li, M. Sun, J. Song, T. Zhang, Y. Zhao, K. Wang, Enhanced adhesion between PEEK and stainless-steel mesh in resistance welding of CF/PEEK composites by various surface treatments, High Perform. Polym. (2021) 095400832110011. https://doi.org/10.1177/09540083211001115.

[32] R. Kolisnyk, M. Korab, M. Iurzhenko, O. Masiuchok, Y. Mamunya, Development of heating elements based on conductive polymer composites for electrofusion welding of plastics, J. Appl. Polym. Sci. 138 (2021) 50418. https://doi.org/10.1002/app.50418.

[33] E. Dahl, H. Schürmann, C. Mittelstedt, A tailored heating element for resistance welding of complex shaped joining surfaces, J. Thermoplast. Compos. Mater. (2020) 089270572098204. https://doi.org/10.1177/0892705720982045.

[34] I.G. Araújo, L.F. P Santos, L.F.B. Marques, J.F. Reis, S.D. B de Souza, E.C. Botelho, Influence of environmental effect on thermal and mechanical properties of welded PPS/carbon fiber laminates, Mater. Res. Express. 6 (2019) 105337. https://doi.org/10.1088/2053-1591/ab3acd.

[35] X. Cui, D. Wang, S. Wang, J. Wei, L. Tian, Y. Deng, X. Xiong, Improved resistance-welded joints of thermosetting composites via flame-grown carbon nanotube, J. Adhes. Sci. Technol. 35 (2021) 1357–1371. https://doi.org/10.1080/01694243.2020.1846899.

[36] V. Rohart, L. Laberge Lebel, M. Dubé, Improved adhesion between stainless steel heating element and

PPS polymer in resistance welding of thermoplastic composites, Compos. Part B Eng. 188 (2020) 107876. https://doi.org/10.1016/j.compositesb.2020.107876.

[37] M. Russello, E.K. Diamanti, G. Catalanotti, F. Ohlsson, S.C. Hawkins, B.G. Falzon, Enhancing the electrical conductivity of carbon fibre thin-ply laminates with directly grown aligned carbon nanotubes, Compos. Struct. 206 (2018) 272–278. https://doi.org/10.1016/j.compstruct.2018.08.040.

[38] X. Yao, S.C. Hawkins, B.G. Falzon, An advanced anti-icing/de-icing system utilizing highly aligned carbon nanotube webs, Carbon N. Y. 136 (2018) 130–138. https://doi.org/10.1016/j.carbon.2018.04.039.

[39] M. Russello, G. Catalanotti, S.C. Hawkins, B.G. Falzon, Welding of thermoplastics by means of carbon-nanotube web, Compos. Commun. 17 (2020) 56–60. https://doi.org/10.1016/j.coco.2019.11.001.

[40] P. Hojati-Talemi, S. Hawkins, C. Huynh, G.P. Simon, Understanding parameters affecting field emission properties of directly spinnable carbon nanotube webs, Carbon N. Y. 57 (2013) 388–394. https://doi.org/10.1016/j.carbon.2013.01.088.